JPMTR-2224
DOI 10.14622/JPMTR-2224
UDC 621.31:546.34:655.224

Research paper | 173
Received: 2022-10-11
Accepted: 2023-03-03

Li-ion battery anodes printed by rotogravure

Alexandra Pekarovicova, Kevin Matthew, Jorge Vicco Mateo, Kholoud Al-Ajlouni and Paul D. Fleming

Center for Printing and Coating Research,
Western Michigan University, Kalamazoo, MI

a.pekarovicova@wmich.edu

Abstract

Inks for Li-ion battery anodes were formulated for printing with the rotogravure printing process. Graphite powders with different particle sizes were used as conductive materials along with nanoparticle carbon black fillers. As polymer binders, polyvinylidene fluoride (PVDF) (commercial names Kureha 9100 and Kureha 9300) and polyvinyl pyrrolidone (PVP) were tested. Inks were printed using proprietary gravure engraving. Ink solid content of 30–70 % was examined. At 70 % solids, ink layers were 25–27 μm thick with mass loading of 2.1–2.5 mg/cm^2. A solids content of 50 % was found the highest that produced a smooth uniform film. Half cells were made using print with 1000 μm holes or they were bar coated. Half cells were charged and discharged in order to measure irreversible capacity loss (ICL). Inks with mixed binders Kureha/PVP were performing better than sole polymers. Half-cell testing revealed that PVP as a sole binder has not good electrical performance, thus it was mixed with PVDF. The ICL was lower when mixed PVDF/PVP binder was employed in anode ink.

Keywords: printed batteries, ink formulation, half cell, capacity, irreversible capacity loss

1. Introduction and background

Due to the increasing impact of oil pollution on the environment (CO_2 production and liquid spills), more automobile and many other industries have turned to electric item manufacturing. Therefore, the production of more energy-efficient and environmentally friendly batteries has become a hot topic at the moment. The traditional lead-acid battery is bulky and heavy, but the printing processes can produce much thinner and lighter batteries to provide power for wearable devices, flexible displays, and smart labels among others (Costa, Gonçalves and Lanceros-Méndez, 2020; Khan, Lorenzelli and Dahiya, 2015). With the advent of printed electronics, flexible batteries have undergone rapid development in the past ten years.

The use of printing processes in battery manufacturing can lead to mass production of flexible batteries (Arduini, et al., 2016). Printing can produce flexible batteries with different design patterns, and their multilayer printing stack can shape the geometry and structure of the battery and improve its electrochemical performance. There are usually two types of the printed structures of printed batteries, such as stack or sandwich architecture and the coplanar or parallel architecture. Components used are anode, separator, electrolyte, cathode, and current collectors deposited on the flexible substrate (Lanceros-Méndez and Costa, 2018). Most of the batteries are manufactured in a stacked structure (Willert, Meuser and Baumann, 2018), while some are made in a coplanar configuration (Kim, et al., 2015). The advantage of coplanar configuration is that it, among other manufacturing processes, can be made using the screen-printing process and the total thickness of the battery can be reduced to 0.5 mm. Its disadvantage is that its discharge current and area ratio charge density is lower, and it has a higher internal resistance.

Currently, many researchers are focusing on screen printing of battery electrodes. This printing technology can use high viscosity inks for printing, which allows them to have good coverage on different materials, such as copper foil (Vicco Mateo, 2022), or plastic (Zhao and Wu, 2019), which are suitable for printing lithium-ion battery electrodes (Khan, Lorenzelli and Dahiya, 2015). Based on the size required to print battery electrodes, the amounts of active materials, the roughness of the electrode layer, and the thickness of each layer of the battery can be modified. There have been many studies using printing methods such as gravure printing, flexographic printing, screen printing, extrusion printing, and inkjet printing to explore

battery electrode production (Søndergaard, Hösel and Krebs, 2013, Hübner, et al., 2015) as well as attempts to print electrolyte (Hübner, et al., 2022). Lithium metal powder-based inks, which contain lithium metal powder, polymer binders, and other conductive materials can be used in anode printing. In general, the advantages of printed batteries are based on mature printing technology, and the fact that they are light, flexible, low-cost, can be mass-produced, customizable, and more environmentally friendly.

Research in the printed batteries based on gravure printing showed that the quality of the gravure printing layer mainly depends on several physical parameters such as ink, substrate, and process. To enable the mass production of batteries through gravure printing, the study was done using carbon coated $Zn_{0.9}Fe_{0.1}O$ (encapsulated in a thin film of carbon) as a reference alloying material (Bresser, et al., 2013). With the water-based electrode inks, 2-propanol can be used as a cosolvent to reduce the excessive surface tension of water-based inks in combination with corona pretreatment of the substrate for increased surface energy and thus ink adhesion (Biscay, Ghoufi and Malfreyt, 2011). Using the gravure printing process, multiple layers can be deposited, and the multilayer method applied is able to obtain the required mass loading (about 1.7 mg cm^{-2}) to achieve high homogeneity of the gravure printed layer, and its highly reproducible electrochemical performance up to 400 life cycles (Montanino, et al., 2021).

Printing inks for anode and cathode layers contain active materials, such as graphite and graphene, and active fillers such as nanocarbons, and resins or binders, which are selected based on ink – chemistry whether ink is solvent, or water-based. Graphene can be doped by ball milling technique, and can be combined with silicon, silicon oxide, and iron oxide for improved performance (Yu, et al., 2022). Resins can include lithiated polyacrylic acid, or polyvinylidene fluoride (PVDF) of different degrees of polymerization. The advantage of printing batteries is that layers of variable thickness can be produced. Printed layers are flexible, and they can be integrated into various substrates and devices. Printing technologies make it possible to easily scale up the products (Costa, Gonçalves and Lanceros-Méndez, 2020). Printed layers should be thick, preferably up to 100 µm and therefore screenprinting is the process of choice (Rassek, et al., 2019). There was not much information found specifically in gravure printing of anodes and cathodes, which calls for need to explore gravure process for printing these features for batteries.

In this work, the aim was to formulate rotogravure printing inks for anodes and evaluate their printability in terms of print uniformity, thickness of the layers and ultimately, half-cell battery performance.

2. Materials and methods

The substrate for anode Li-ion battery printing was copper foil from MTI Co., with caliper of 9 µm. Its surface roughness was 0.32 µm as measured by Bruker white light interferometry. Sheet resistivity of Cu foil was measured using SRM-232 sheet resistance meter with four-point probe and it was 0.0018 Ω/sq. Surface energy of copper foil was measured via contact angle with water: 87.2 ± 1.3° and hexadecane: 3.3 ± 0.1°, as well as surface tension of water via pendant drop measurement: 71.1 ± 0.6 mN/m; surface tension of hexadecane via pendant drop measurement: 24.5 ± 0.3 mN/m. These values were plugged into the Owens–Wendt equation and surface energy of copper was estimated to be 26.5 ± 0.7 mN/m.

A Thinky Mixer AR 100 (THINKY Co., Tokyo Japan) was employed for mixing the inks. As the conductive graphite powders, Philips 5 µm, 10 µm, 15 µm (Philips 66, Houston, Texas) and Mage 3 graphite (Hitachi Chemical, Sakuragawa, Japan), and conductive nanoparticle carbon black filler (CB 4400 or C45) with particle size of 20 nm were used. The PVDF from Sigma Aldrich with different degrees of polymerization and commercial names Kureha 9100, Kureha 9300 (Kureha Co., Japan) with molecular weights of 2.8×10^5 to 1×10^6 was dissolved in N-methyl-2-pyrrolidone (NMP) solvent and used as the vehicle. In some inks, a polyvinylpyrrolidone (PVP) with molecular weight of 10 000 or polyvinylpyrrolidone/polyvinylidene fluoride mix of binders (PVP/PVDF) was employed. Rheology of finished inks was evaluated on an Anton Paar MRC302 rheometer.

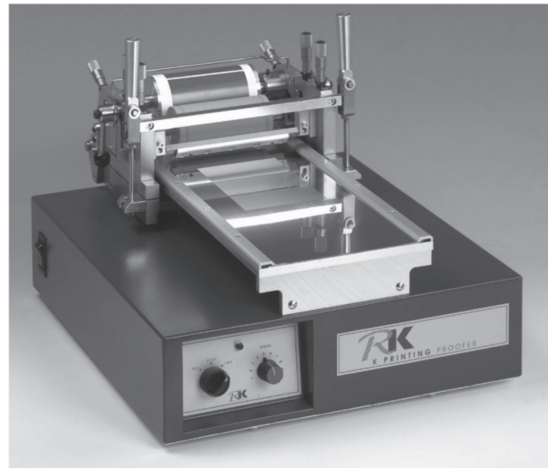

Figure 1: Gravure RK-proofer

Printing was done on Cu foil using a gravure RK gravure K-proofer (Figure 1), which uses a flat plate as an image carrier. The gravure plate for the RK gravure K-proofer was engraved by WRE/ColorTech (Greensboro, NC, USA) with proprietary engraving at 75 LPI. A plate was

engraved with 1000, 500, 250 and 125 µm circular hole shaped nonimage areas. Detail of 500 µm nonimage area is shown in Figure 2 and white-light interferometry detail is shown at Figure 3, showing depth of cells at 75 µm and the cell opening in one direction of the 1000 µm designed hole was measured at 1194 µm. Engraving was done by hybrid process of laser ablation and chemical etching. Such holes in the printed image improve the battery performance at high C rates and reduce lithium dendrites that collect on the electrodes.

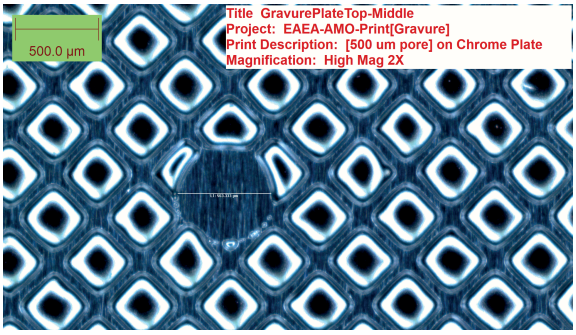

Figure 2: Detail of new gravure engraved plate (by WRE Color/Tech, Greensboro, NC, USA) with 500 µm nonimage area (circular hole)

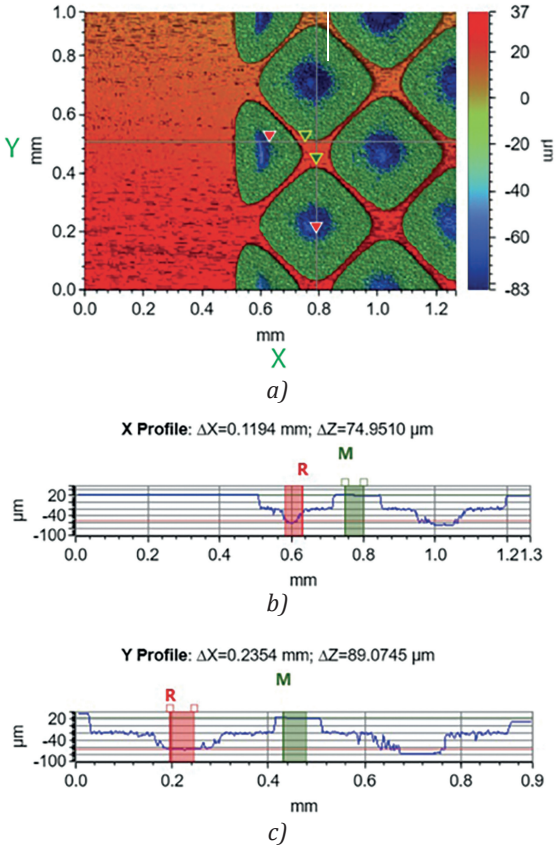

Figure 3: White-light interferometry of gravure engraved plate: view from above (a), cell profile in X-direciton (b), and in Y-direction (c)

Precisely controlled porous architecture of electrodes is necessary for fast charging cells. Fast charging requires electrodes with high porosity and low tortuosity enabling fast electrolyte transport and at the same time prevent lithium plating (Mijailovic, et al., 2021). Thus, circular holes, or non-image areas were designed on printed electrodes with the aim to create so called secondary porosity. Secondary porosity was found useful in suppressing Li dendrites formation in graphite electrodes at fast charging rates (Emani, et al., 2022, Palaniappan, et al., 2022).

The profile of the plate and ink films was prepared on a Bruker white-light interferometry instrument. Image analysis of printed ink films was done using PAX-it 2 software.

In order to test irreversible capacity loss (ICL) of anodes, half coin cells were constructed (Figure 4) in a glove box to avoid moisture and oxygen damage. A half-cell contains a conductive electrode, conductive electrolyte and a current collector. Reversible/irreversible capacity and stability of the electrode was obtained from the galvanostatic cycling technique (Figure 5).

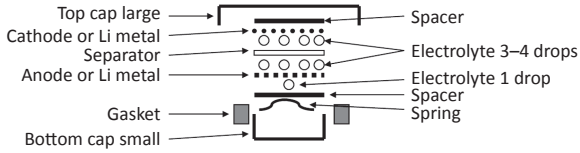

Figure 4: Schematic of half coin cell (Jansen, et al., 2018)

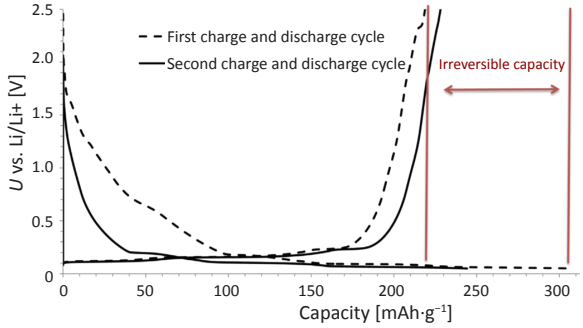

Figure 5: Illustration of ICL determination (Libich, et al., 2017)

3. Results and discussion

Anodes for Li-ion battery electrodes were printed with long-chain PVDF polymer inks. As active materials, graphite powders of different particle sizes were employed. Graphite powders are deemed to be efficient and economical conductive materials; thus, they were considered very suitable for this work. At this stage, particle size of the graphite powders from 5 µm to about 22 µm was assessed; thus only the graphite part

Table 1: Gravure anode ink formulation

Ink	Ink composition Active material	Conductive additive	Binder	Ink formulation (graphite/CB/PVDF)
1	Phillips graphite powder (5 µm)	Nanoparticle carbon black filler (CB)	PVDF or PVP	92/2/6
2	Phillips graphite powder (10 µm)			
3	Phillips graphite powder (15 µm)			
4	Mage 3 graphite powder (22.4 µm)			

of the ink formulation was changed, and the rest of the formulation was held the same (Table 1). Solid content of all four inks was kept at 50 %, because higher solid content could not be printed uniformly on the designed structure of gravure plate. As a binder, Kureha 9300 PVDF was used and as a solvent, NMP was employed. The PVDF is a highly non-reactive thermoplastic fluoropolymer. It is a special polymer used in applications requiring the highest purity as well as resistance to solvents, acids, and hydrocarbons with excellent mechanical properties. It was selected because it is a known binder for carbon electrodes in supercapacitors and other electrochemical applications. The NMP was selected as a solvent for this system because of its high chemical and thermal stability, and compatibility with many solvents such as alcohols, ketones, chlorinated and fluorinated hydrocarbons.

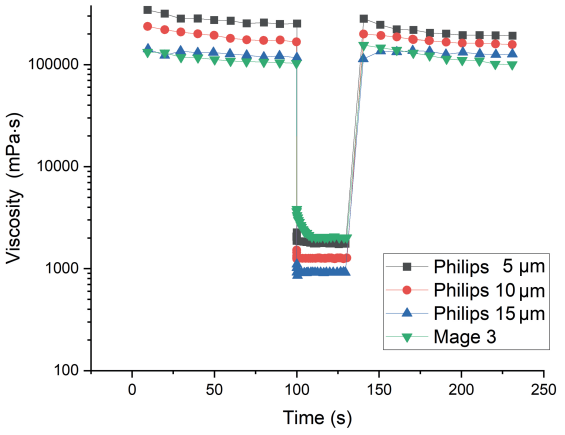

Figure 6: Rheology testing of PVDF inks with graphite particle size 5 µm to 22.4 µm and solid content of 50 %; testing conditions 0.1 s^{-1} → 200 s^{-1} → 0.1 s^{-1} were applied for thixotropic behavior testing

Formulated inks were tested for their rheological properties (Figures 6 and 7). Viscosity of polymer suspensions usually increases with increased degree of polymerization, and higher solids content. At certain composition, its viscosity is reduced by increasing the applied shear rate, because the bonds between the polymer chains are broken (Triantafillopoulos, 1988). Tendency of ink to lose viscosity when stirred is called pseudoplasticity. This property favors the ink in the moment of printing because it flows more easily. When the stress or shear rate is decreased, the viscosity of polymer suspensions or inks is regained, e.g., when ink is printed its viscosity increases again, which helps the ink to set on the substrate and create required print features. Not all inks set at the same speed. The speed at which the structure is restored is related to thixotropy. Figure 6 shows that all the tested inks after increased shear drastically decreased in viscosity, but after returning to the original shear rate, the viscosity was regained rather quickly, which shows that all of those inks display only weak thixotropic behavior. The highest viscosity was found for ink with Philips 5 µm, while the inks with Mage 3 and Philips 15 µm had the lowest viscosity. Pseudoplastic behavior of the inks was confirmed in regime of shear rate of 0.1–200 s^{-1} for the flow curve. All of inks were shear-thinning (Figure 7).

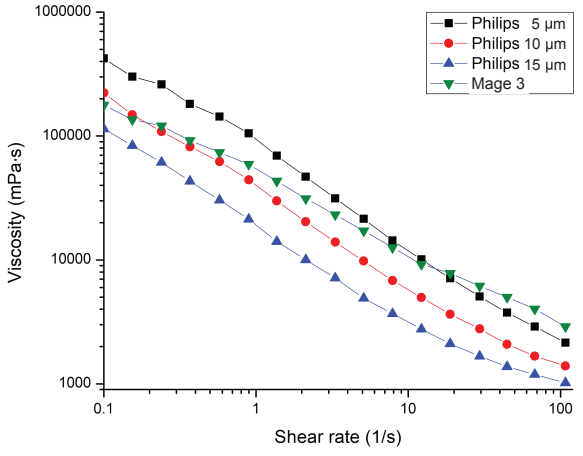

Figure 7: Viscosity change of PVDF inks with graphite particle size of 5 µm to 22.4 µm and solid content of 50 % with shear rate; shear rate of 0.1–100 s^{-1} was applied

All of these inks were printed on an RK gravure K-proofer (see Figure 1), and these experiments showed that ink containing graphite powder with 5 µm particle size exhibited the best print quality. The reason may be that the 5 µm graphite particle size could deposit the ink film with lowest primary porosity and the best ink film integrity. Also, 5 µm particle size of graphite probably enables easiest ink release from gravure image carrier. Overall, all applied PVDF inks seem to have too high viscosity for rotogravure printing process. Therefore, we wanted to experiment

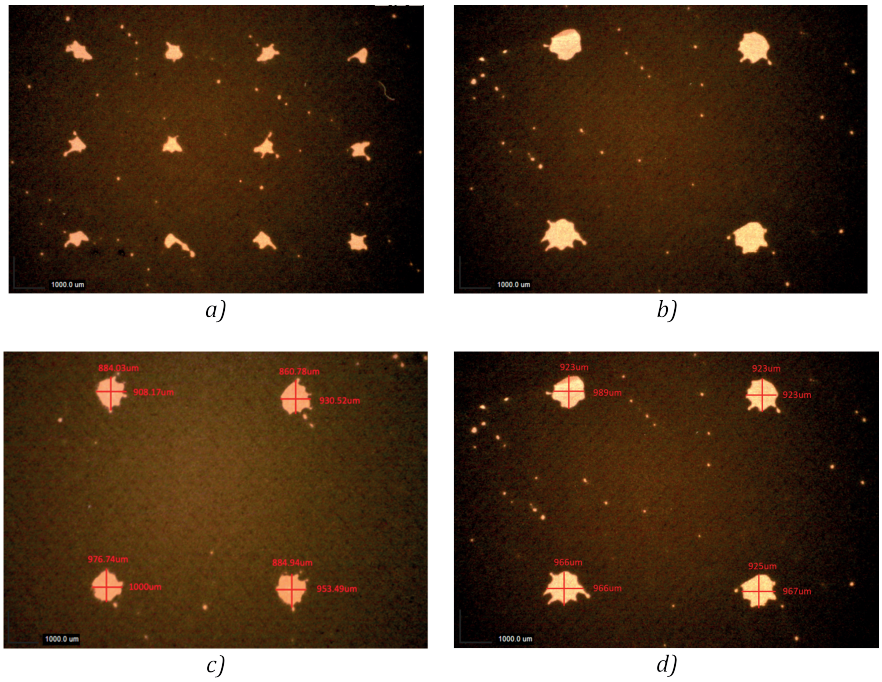

Figure 8: Illustration of printed non-image areas (holes) 500 µm (a), and 1000 µm (b) with graphite 5 µm and P5/CB/PVP ink (a and b); and 1000 µm holes printed with P5/CB/PVP-PVDF Kureha 9100 (c) and P5/CB/PVP-PVDF Kureha 9300 (d)

with lower ink viscosity, for which a new PVP resin at 10 000 molecular weight was tested to disperse graphite and nanocarbon active materials. Inks with 30–72 % solids were formulated with graphite from Philips (P5) with size of 5 microns, and conductive filler CB 4400 with the ratio of ingredients Philips P5, CB 4400 and PVP of 80/5/15. As a solvent, ethanol or NMP were used. Ethanol was evaporating too fast, thus NMP was chosen as a more suitable solvent. The average surface tension of NMP ink with 70 % solids was 39.4 mN/m and average contact angle with copper surface was 40.8° (data not shown). At 70 % solids, ink layers were 25–27 µm thick with mass loading of 2.1–2.5 mg/cm^2 (data not shown). PVP inks showed excellent dispersing characteristics and improved print quality when compared with PVDF ink prints.

Printed inks with PVP resin are shown in Figures 8a and 8b. Gravure prints with NMP as a solvent were easier to work with than using inks with water or ethanol as a solvent. Designed circular holes with diameter of 1000 µm were resulting in printed circles of 846 ± 20 µm in diameter, while 500 µm circular holes were printed with 219 ± 11 µm diameter, smaller than those shown in Figure 3 (Figures 8a and 8b). Primary porosity of printed electrodes mostly depends on different particle sizes of active material, in our case graphite of different particle sizes of 5–15 µm. Designed circular holes, or nonimage areas are responsible for secondary porosity.

Printed ink films on copper foil were used to construct half coin cells according to Figure 4. Half cells were used to assess reversible/irreversible capacity and stability of printed anodes. Irreversible capacity loss of half coin cells made with PVP inks was too high and half cells did not have sufficient electrical performance. Thus, in the next step PVP was mixed with PVDF – Kureha 9100 or Kureha 9300 and half cells were made again. The first attempts showed that mixing Kureha and PVP resins is possible, so far 2 : 1 ratio was tested, and inks exhibited uniform prints. Their performance in terms of ICL was tested again (Figure 9). Inks were bar coated, not gravure printed to ensure higher thickness of layers than what was possible to achieve with gravure printing. Figure 9 should be compared with Figure 5.

From Figures 10 and 11, it can be seen that performance of mixed PVP/PVDF inks was greatly improved compared to PVP or PVDF alone, and mixed PVP/PVDF achieved actually better performance and suffered from less ICL than inks made with sole Kureha 9100 or 9300. The PVP is known to have excellent dispersing properties. The macromolecule of PVP contains strong polar lactam hydrophilic groups and C–C long-chain lipophilic groups, which can be well compatible with a variety of solvents and can be coated on the surface of particles to form a good dispersion effect through steric hindrance. Introducing PVP, a polymer with an amphiphilic structure, onto the surface of graphite can significantly improve the dispersion properties

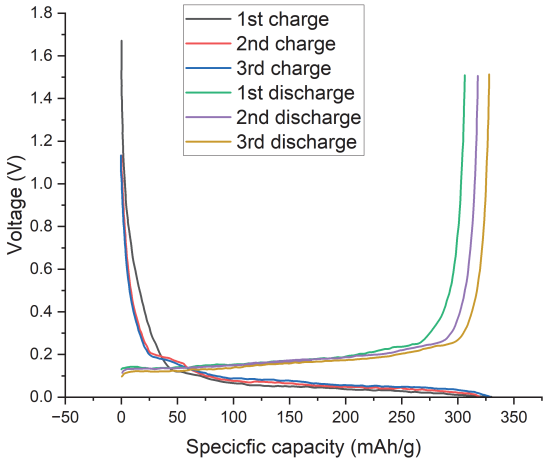

Figure 9: Irreversible capacity loss of half cell with anode ink formulation P5/CB/(PVP + PVDF 9100) = 80/5/(5+10); mass loading: ≈5.26 mg/cm², porosity: ~35 %

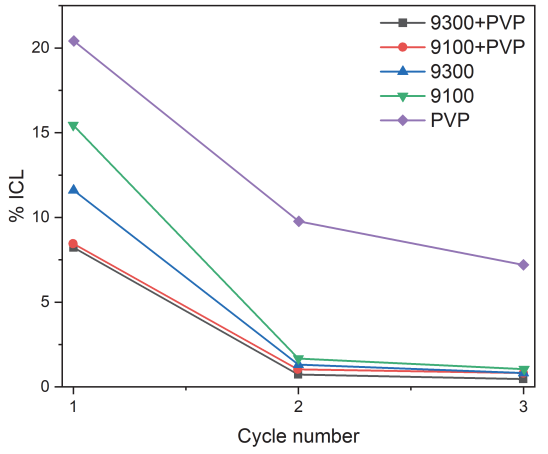

Figure 10: Comparison of half-cell battery performance (as ICL) with resins: sole PVP, two types of sole PVDF and the corresponding combination of PVP/PVDF

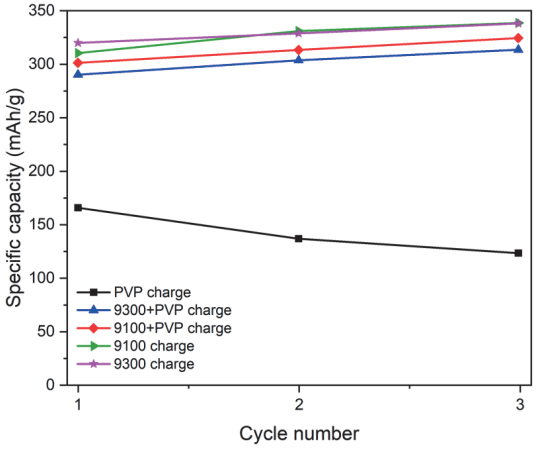

Figure 11: Capacity of bar coated samples; test conditions, formation: 0.01–1.5 V, ± 0.1 C

of graphite in water, or organic solvents. Therefore, PVP can be used as dispersant for Li-ion battery electrode inks and other conductive materials (Bollen, 2021; Li, 2022). This is most likely the reason that PVP enhances the electrical performance of printed anodes in mixed PVP/PVDF inks. PVP with molecular weight around 10 000 creates low viscosity dispersions, which can be suitable for gravure printing, but as a sole binder it does not have sufficient mechanical properties needed for battery architecture. PVDF has large molecular weight (500 000–1 000 000) and its macromolecules create highly viscous dispersions, suited better for screen printing than for gravure printing.

Besides optimized viscosity, mechanical and dispersing properties, mixed PVP/PVDF suspensions exhibit intermolecular forces, beneficial for improved electrical performance. When the two binders PVP and PVDF (Figure 12) were mixed at the ratio of 4 : 1 and allowed to stand for 0–24 hours, obvious darkening of color was observed in the mixtures.

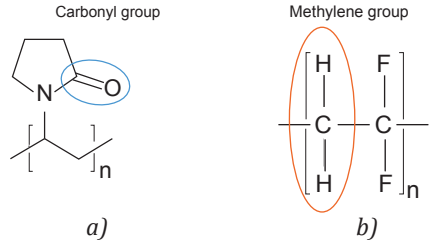

a) *b)*

Figure 12: Illustration of position of carbonyl group of PVP (a) and methylene group of PVDF (b)

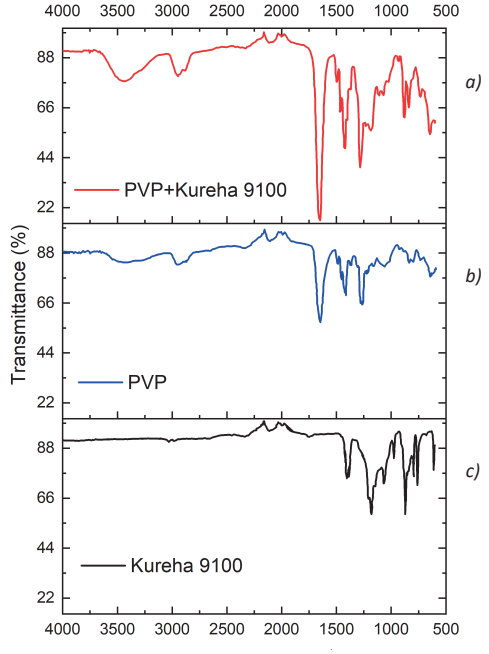

Figure 13: FTIR spectra of PVP + Kureha 9100 (a), PVP (b), and Kureha 9100 (c)

FTIR was performed on the mixtures to understand what may be contributing to color change and change in ink electrical performance. Binders were dried and ground, and FTIR was performed from 500 cm^{-1} to 4 000 cm^{-1} (Figure 13). The FTIR spectrum showed broadening of O–H groups at 3 434 cm^{-1}, and 3 426 cm^{-1} which could occur due to stretching of O–H bonds. Stretching of C–H groups at 3 000 cm^{-1} and C=O group at 1 652 cm^{-1} was also observed, which strongly suggests the formation of hydrogen bonds between C=O groups of PVP and methylene groups of PVDF (see Figure 12), which could lead to improved electrical performance of printed anodes. Similar behavior was found for PVDF Kureha 9100 and Kureha 9300 in the mixture with PVP.

4. Conclusions

Gravure inks for battery anodes were formulated and printed on a laboratory K-proofer with proprietary engraving. It was found that PVP inks showed good printability, but poor battery performance. Using mixed PVP/PVDF 9300 or PVP/PVDF 9100 binder combination could effectively improve battery performance without significantly sacrificing the printability.

From several graphites having particle sizes between 5 µm to 22.4 µm, graphite with 5 µm particle size was the most suitable for gravure printing. The PVDF inks under commercial name Kureha 9100 or 9300 with NMP solvent showed best specific capacity during three charging/discharging cycles, and ICL was even lower when these PVDF polymers were mixed with PVP.

The FTIR study showed that methylene group ($-CH_2$) and carbonyl groups (C=O) demonstrated lower transmittance and O–H groups showed stretching. This clearly suggests the formation of hydrogen bonds. Hence, the hydrogen bonds formed between the methylene groups and carbonyl groups could be a contributing factor to the reduction of ICL in mixed binder printed anodes.

Acknowledgement

This work was made possible by funding through DOE Advanced Manufacturing Office (DE-EE0009111) by Wu Q., et al.: Enabling Advanced Electrode Architecture through Printing and Pekarovicova A.: GEF-PGSF Gravure Day 2021 grant.

References

Arduini, F., Scognamiglio, V., Moscone, D. and Palleschi, G., 2016. Electrochemical biosensors for chemical warfare agents. In: D.P. Nikolelis and G.-P. Nikoleli, eds. *Biosensors for security and bioterrorism applications.* Cham, Switzerland: Springer. https://doi.org/10.1007/978-3-319-28926-7_6.

Biscay, F., Ghoufi, A. and Malfreyt, P., 2011. Surface tension of water-alcohol mixtures from Monte Carlo simulations. *The Journal of Chemical Physics,* 134(4): 044709. https://doi.org/10.1063/1.3544926.

Bollen, D., Agfa-Gevaert NV., 2021. *A metallic nanoparticle dispersion*. Pat. EP 3 287 499 B1.

Bresser, D., Mueller, F., Fiedler, M., Krueger, S., Kloepsch, R., Baither, D., Winter, M., Paillard, E. and Passerini, S., 2013. Transition-metal-doped zinc oxide nanoparticles as a new lithium-ion anode material. *Chemistry of Materials,* 25(24), pp. 4977–4985. https://doi.org/10.1021/cm403443t.

Costa, C.M., Gonçalves, R. and Lanceros-Méndez, S., 2020. Recent advances and future challenges in printed batteries. *Energy Storage Materials*, 28, pp. 216–234. https://doi.org/10.1016/j.ensm.2020.03.012.

Emani, H.R.K.M., Palaniappan, V., Maddipatla, D., Bazuin, B.J., Wu, Q. and Atashbar, M.Z., 2022. Novel laser patterned MXene based anodes for high capacity fast charging Li-ion batteries. In: *2022 IEEE Sensors*. Dallas, TX, USA, 30 October – 2 November 2022. IEEE. https://doi.org/10.1109/SENSORS52175.2022.9967280.

Hübner, G., Krebs, M., Rassek, P. and Willfahrt, A., 2015. Printed batteries, overview, status, recent developments, future perspectives. In: P. Gane, ed. *Advances in Printing and Media Technology: Proceedings of the 42nd International Research Conference of iarigai.* Helsinki, Finland, 6–9 September 2015. Darmstadt: iarigai.

Hübner, G., Krebes, M., Cirstea, L. and Kolesova, A., 2022. Printable electrolyte for printed batteries. In: C. Ridgway, ed. *Advances in Printing and Media Technology: Proceedings of the 48th International Research Conference of iarigai.* Greenville, SC, USA, 18–21 September 2022. Darmstadt: iarigai. https://doi.org/10.14622/Advances_48_2022_14.

Jansen, A., Dunlop, A., Polzin, B. and Trask, S., 2018. Cell analysis, modeling, and prototyping (CAMP) facility electrode and cell development for fast charge applications: BAT 371. In: *2018 Vehicle Technologies Office Annual Merit Review*. Arlington, VA, 18–21 June 2018. Washington, DC: US DOE Vehicle technologies office.

Khan, S., Lorenzelli, L. and Dahiya, R.S., 2015. Technologies for printing sensors and electronics over large flexible substrates: a review. *IEEE Sensors Journal,* 15(6), pp. 3164–3185. https://doi.org/10.1109/JSEN.2014.2375203.

Kim, J.-S., Ko, D., Yoo, D.-J., Jung, D.S., Yavuz, C.T., Kim, N.-I., Choi, I.-S., Song, J.Y. and Choi, J.W., 2015. A half millimeter thick coplanar flexible battery with wireless recharging capability. *Nano Letters,* 15(4), pp. 2350–2357. https://doi.org/10.1021/nl5045814.

Lanceros-Méndez, S. and Costa, C.M. eds., 2018. *Printed batteries: materials, technologies and applications*. Hoboken, NJ: John Wiley & Sons.

Li, L., 2022. *Application of PVP dispersant in lithium battery industry*. [online] Tycorun Energy. Available at: <https://www.takomabattery.com/application-of-pvp-dispersant-in-lithium-battery-industry/> [Accessed January 2022].

Libich, J., Máca, J., Vondrák, J., Čech, O. and Sedlaříková, M., 2017. Irreversible capacity and rate-capability properties of lithium-ion negative electrode based on natural graphite, *Journal of Energy Storage*, 14(3), pp. 383–390. https://doi.org/10.1016/j.est.2017.03.017.

Mijailovic, A., Wang, G., Li, Y., Yang, J., Lu, W., Wu, Q. and Sheldon, B.W., 2021. Quantifying the role of reaction inhomogeneity on optimizing capacity and reducing lithium plating in conventional and architectured electrodes during fast charging. In: *MRS 2021 Fall Meeting & Exhibit: SYMPOSIUM BI01*. Boston, MA, USA, 30 November – 7 December 2021. Materials Research Society.

Montanino, M., Sico, G., De Girolamo Del Mauro, A., Asenbauer, J., Binder, J.R., Bresser, D. and Passerini S., 2021. Gravure-printed conversion/alloying anodes for lithium-ion batteries. *Energy Technology,* 9(9): 2100315. https://doi.org/10.1002/ente.202100315.

Palaniappan, V., Maddipatla, D., Ahmadi, S., Emani, H.R.K., Wang, G., Hanson, T., Narakathu, B.B., Bazuin, B., Wu, Q. and Atashbar, M., 2022. Improving registration accuracy of multilayer screen-printed graphite electrodes with secondary pore networks for fast charging lithium-ion batteries. In: *2022 IEEE International Conference on Flexible and Printable Sensors and Systems (FLEPS)*. Vienna, Austria, 10–13 July 2022. IEEE. https://doi.org/10.1109/FLEPS53764.2022.9781519.

Rassek, P., Steiner, E., Herrenbauer, M. and Claypole, T.C., 2019. The effect of electrode calendering on the performance of fully printed Zn|MnO_2 batteries. *Flexible and Printed Electronics,* 4(3): 035003. https://doi.org/10.1088/2058-8585/ab38e2.

Søndergaard, R.R., Hösel, M. and Krebs, F.C., 2013. Roll-to-roll fabrication of large area functional organic materials. *Journal of Polymer Science Part B: Polymer Physics,* 51(1), pp. 16–34. https://doi.org/10.1002/polb.23192.

Triantafillopoulos, N., 1988. *Measurement of fluid rheology and interpretation of rheograms*. 2nd ed. [pdf] Caltec Scientific, Inc. Available at: <http://www.kaltecsci.com/rheology.pdf> [Accessed January 2022].

Vicco Mateo, J., Matthew, K., Pekarovicova, A. and Fleming, P.D., 2022. Inks for Li-ion battery anodes printed by rotogravure. In: C. Ridgway, ed. *Advances in Printing and Media Technology: Proceedings of the 48th International Research Conference of iarigai.* Greenville, SC, USA, 18–21 September 2022. Darmstadt: iarigai. https://doi.org/ 10.14622/Advances_48_2022_04.

Willert, A., Meuser, C. and Baumann, R.R., 2018. Printed batteries and conductive patterns in technical textiles. *Japanese Journal of Applied Physics,* 57(5S): 05GB02. https://doi.org/10.7567/JJAP.57.05GB02.

Yu, S., Guo, B., Zeng, T., Qu, H., Yang, J. and Bai, J., 2022. Graphene-based lithium-ion battery anode materials manufactured by mechanochemical ball milling process: a review and perspective. *Composites Part B*, *Engineering*, 246: 110232. https://doi.org/10.1016/j.compositesb.2022.110232.

Zhao, Z. and Wu, H., 2019. Monolithic integration of flexible lithium-ion battery on a plastic substrate by printing methods. *Nano Research*, 12(10), pp. 2477–2484. https://doi.org/10.1007/s12274-019-2471-z.